Pergamon

Atmospheric Environment Vol. 29, No. 18, pp. 2541–2546, 1995

1352-2310/95 $9.50 + 0.00

1352-2310(95)00194-8

TECHNICAL NOTE

COMPUTATION OF GLOBAL PHOTOCHEMISTRY WITH SMVGEAR II

MARK Z. JACOBSON

Department of Civil Engineering, Stanford University, Stanford, CA 94305-4020, U.S.A.

(*First received* 5 *January* 1995 *and in final form* 31 *March* 1995)

Abstract—A computer model was developed to simulate global gas-phase photochemistry. The model solves chemical equations with SMVGEAR II, a sparse-matrix, vectorized Gear-type code. To obtain SMVGEAR II, the original SMVGEAR code was modified to allow computation of different sets of chemical reactions for urban, free-tropospheric, and stratospheric regions during the same model run. SMVGEAR was also modified to allow grid cells in each region of the atmosphere to be reordered according to stiffness of the chemical equations, each time interval. Reordering speeds solutions by a factor of more than two compared to not reordering. Two 30 day simulations of chemistry coupled (with feedback) to radiation field calculations over a global grid, were performed. In one simulation, results were obtained for 49,680 grid cells (15-layers general circulation model grid), and in the other, results were obtained for 96,048 cells (29-layer grid). In both simulations, 200 "urban" (assumed below 900 mb) chemical equations were solved, 169 "free tropospheric" (225–900 mb) equations were solved, and 115 "stratospheric" (above 225 mb) equations were solved. The times required for the two 30 day simulations on a single processor of a Cray 90 were 6.2 and 11.6 h, respectively, at an average speed of approximately 362 megaflops.

Key word index: Gear code, photochemistry, global modeling, air pollution, ordinary differential equations.

1. INTRODUCTION

Models that simulate atmospheric photochemistry require the use of a stiff-ordinary differential equation solver. Because the number of model grid cells are often large and integration periods are often long, the numerical solver must be computationally fast. Also, the residual error from the solver must be small. Because most accurate solvers are relatively slow, modelers have often reduced computer time by either reducing the size of the modeling domain, reducing the number of species and reactions solved, or simplifying the chemical solver.

For example several excellent tropospheric or stratospheric chemical modeling studies have been carried out in two, instead of three, dimensions, because computer time was limited (e.g. Crutzen *et al.*, 1978; Logan *et al.*, 1981; Derwent, 1982; Isaksen and Hov, 1987; Austin, 1991; Hough, 1991; Kanakidou *et al.*, 1991; Garcia and Solomon, 1983, 1994; Ko *et al.*, 1993; Tie *et al.*, 1994; Strand and Hov, 1994). In addition, pioneering three-dimensional studies have often been carried out with either parametrized chemical solvers (e.g. Jacob *et al.*, 1989) or family solvers (e.g. Kaye and Rood, 1989; Rose and Brasseur, 1989; Kao *et al.*, 1990; Lefevre *et al.*, 1994; Elliott *et al.*, 1995).

In order to solve many chemical reactions in a large global grid with a high order of accuracy, either faster computers or faster integrators are required. Recently, Gear's predictor–corrector scheme (Gear, 1971) was modified with sparse matrix and vectorization techniques to obtain a fast integrator (Jacobson 1994; Jacobson and Turco, 1994). The resulting code, SMVGEAR (sparse matrix, vectorized Gear code), achieves over 360 megaflops on one processor of a Cray 90 computer, solves hundreds of chemical rate equations in large model domains, and maintains the accuracy of Gear's original code.

For a copy of this code, please email jacobson@ce.stanford.edu.

For the work described herein, SMVGEAR was modified to solve chemical rate equations over a global grid domain, where the stiffness of the equations varies significantly from place to place and time to time. In addition, SMVGEAR was modified to serially solve different sets of chemical equations for different regions of the atmosphere. For example, stratospheric, free tropospheric, and urban chemistry can be solved during the same model simulation. Specifying different chemical mechanisms for different regions of the atmosphere reduces computational requirements significantly. The modified version of SMVGEAR is called SMVGEAR II.

To simulate global photochemistry, SMVGEAR II was coupled to a radiative transfer model. Optical properties of all photodissociating gases in the model were used to calculate the radiation fields; consequently, feedback between chemistry and radiation occurred. Subsequently, computer timings were performed. In the following sections, SMVGEAR II is discussed and analyzed and computer timings are shown.

2. MODIFICATIONS TO SMVGEAR

2.1. *Description of SMVGEAR*

SMVGEAR is derived from Gear's, predictor–corrector method (Gear, 1971), which was based on the backward differentiation formula (BDF). The BDF can be written as (e.g. Byrne *et al.*, 1977; Hindmarsh, 1983)

$$y_n = h\beta_0 \frac{dy_n}{dt} + \sum_{j=1}^{q} \alpha_j y_{n-j} \quad (1)$$

where y_n is an array of N real variables at time t_n (and n denotes the time step number), $dy_n/dt = f(t_n, y_n)$ is an array of first derivatives for each value of y_n at time t_n, $h = t_n - t_{n-1}$ is the current time step, q is the current order of the method ($1 \leqslant q \leqslant 5$), and α_j and β_0 are scalar multipliers ($\beta_0 > 0$) that depend on the current order. The boundary

conditions, $y_0 = y(t_0)$, define the initial values for the problem.

A solution to equation (1) can be found by solving the modified Newton iterative equation, written as

$$P_n[y_{n(m+1)} - y_{n(m)}] = -y_{n(m)} + h\beta_0 f(t_n, y_{n(m)}) + \sum_{j=1}^{q} \alpha_j y_{n-j} \quad (2)$$

where

$$P_n \approx I - h\beta_0 J_n \quad (3)$$

is a predictor matrix, m is the iteration number, I is the identity matrix, and

$$J_n = J(t_n, y_n) = \left[\frac{\partial f_n^i}{\partial y_n^i}\right]_{i,j=1}^{N} \quad (4)$$

is the Jacobian matrix of partial derivatives.

SMVGEAR uses Gear's solution method; however, sparse matrix and vectorization techniques were applied to improve computational speed significantly. About half of the speedup of SMVGEAR was due to sparse-matrix techniques and half was due to vectorization. The primary sparse-matrix technique was to reorder the matrix of partial derivatives, then to eliminate all subsequent multiplies by zero during matrix decomposition and back substitution. The primary vectorization technique was to divide the grid domain into blocks of approximately 500 grid cells each, then to solve equations in each block together. In such cases, almost every inner loop in the code was vectorized around the grid-cell loop, which had length equal to the number of grid cells in a grid block.

The average size of a grid block in the model was chosen as a compromise between competing factors. For example, when a grid block is large, speed from vectorization increases. However, the number of total operations also increases because more grid cells are tied together whenever a single cell causes many iterations for the block as a whole. A compromise grid block size of 500 was chosen because it is large enough to result in 90% maximum vectorization speed on Cray computers (NAS, 1992) but small enough not to cause too many excess calculations. Nevertheless, excess calculations do occur. Thus, to reduce excess calculations, a method was developed here to reorder grid cells so that cells with similar stiffness are placed in the same grid blocks.

2.2. *Predicting stiffness and reordering grid cells*

In SMVGEAR, grid-cells were grouped arbitrarily into blocks of approximately 500 cells each. For example, a grid with dimensions $40 \times 50 \times 10$ (20,000 grid cells) gave rise to 40 grid blocks. Cells for each block were gathered sequentially, from the southwesternmost corner of the surface layer towards the east, then to the next latitudinal row, and then to the next vertical layer.

While this method of cell-gathering was convenient, it resulted in grid blocks containing groups of adjacent grid cells with different stiffnesses. Examples of where stiffness varies among adjacent cells are regions where sunrise and sunset occur, regions where photodissociation rates differ vertically, and regions where strong concentration gradients occur (such as near emissions).

To reduce excess computations caused by grouping grid cells with varying stiffness together, a technique was developed to regroup grid cells each chemistry time interval according to stiffness. A chemistry time interval is defined as a period during which photochemistry (or photochemistry plus emissions) is solved alone in the model. Before and after a chemistry time interval, transport and other processes are allowed to affect concentrations; however, during a chemistry interval, chemistry is integrated alone, with variable integration time steps. In typical model applications, chemistry time intervals vary between 300 and 1800 s while integration time steps vary between 10^{-8} and 1800 s.

In SMVGEAR II, grid cell stiffness is determined in two ways. First, for each grid cell, except for those in which sunrise occurs during the time interval, stiffness is estimated with

$$S_{k,n} = \frac{1}{N}\sum_{i=1}^{N}\left(\frac{dy_{i,k,n}/dt}{y_{i,k,n} + E_{Ai,k,n}}\right)^2 \quad (5)$$

where $y_{i,k,n}$ and $E_{Ai,k,n}$ are the concentration and absolute error tolerance, respectively, of species i at time n in grid cell k, and N is the order of the matrix of partial derivatives. After the stiffness is estimated for each grid cell with equation (5), the cells are reordered from smallest to largest values of S with the *heapsort* sorting routine (Press *et al.*, 1992), which is an $N \log_2 N$ process. Subsequently, the reordered cells are placed sequentially into grid blocks. Thus, if each grid block contains 500 cells, then the first block will contain the 500 cells with the lowest predicted stiffness values and the last block will contain the 500 cells with the highest predicted stiffness values.

To test the effects of reordering, a 4 h simulation over a global grid domain was performed and statistics were gathered. Figure 1 shows the correlation between the minimum stiffness predicted for each grid block over all time intervals vs the resulting number of matrix back-substitution calls. The number of back-substitution calls correlates positively to stiffness. The figure shows that, in general, the larger the minimum predicted stiffness for the block, the greater the number of back-substitution calls (thus the greater the actual stiffness of equations in the block). Consequently, grouping grid cells that have similar initial stiffnesses reduces excess calculations. To test this hypothesis further, comparisons of results with and without reordering were made. Table 1 compares statistics from global simulations. The table shows that the number of back-substitution calls decreased by a factor of over two when cells were reordered compared to when they were not reordered.

When sunrise occurs, equation (5) is not a good predictor of stiffness since the equation predicts stiffness at the beginning of the interval, before sunrise occurs, and stiffness changes rapidly after sunrise. Instead, sunrise cells are ordered here by time of sunrise. Further, since all sunrise cells face similar stiffness difficulties as each other, they are sequestered into their own blocks. Sunset cells are also given their own blocks. However, they are ordered by stiffness, as predicted from equation (5), since stiffness of sunset cells only decreases between the beginning and end of a time interval. Table 1 shows that the computer time and number of back-substitution calls decreased when cells were sequestered and reordered during sunrise and sunset as opposed to when they were not sequestered or reordered at all.

2.3. *Solving stratospheric, tropospheric, and urban chemistry serially*

The second new feature of SMVGEAR II is a modification that allows it to solve different sets of chemistry for different regions of the atmosphere. For example, many chemical reactions that are important in the stratosphere are not so important in the troposphere. Similarly, many reactions that are important in urban regions are not so important in the free troposphere or stratosphere.

The chemical mechanism used for urban air consist of 200 inorganic and organic reactions (176 kinetic and 24 photolysis reactions). The tropospheric mechanism consists of 169 reactions (147 kinetic and 22 photolysis), which include all the urban reactions except for aromatic reactions. Finally, the stratospheric mechanism consists of 115 reactions (81 kinetic and 34 photolysis), which include inorganic chemistry, light organic chemistry, and chlorine and bromine chemistry. Most reactions in all three mechanisms were

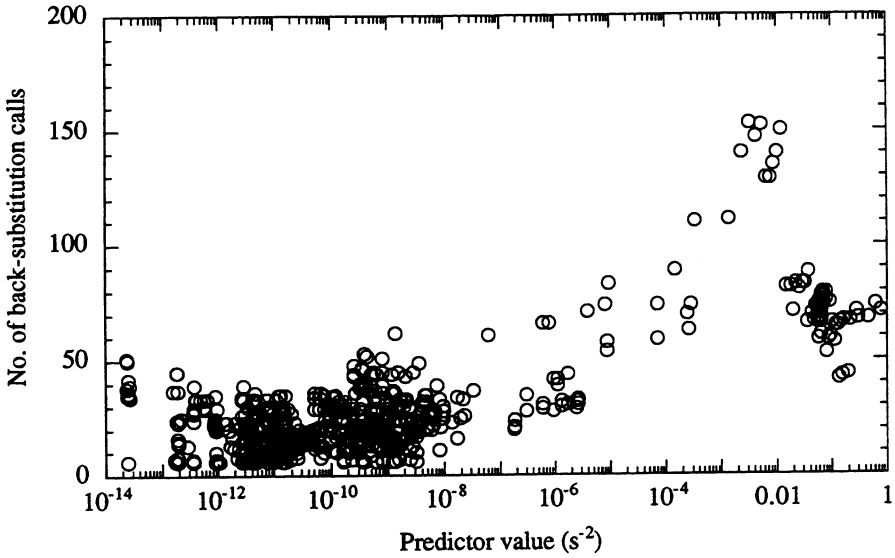

Fig. 1. Number of back-substitution calls for a grid block during a time interval as a function of the smallest stiffness predictor value among all grid cells in the block.

Table 1. Number of matrix back-substitution calls, matrix decomposition calls, and integration time steps required for chemistry during three 4 h global simulations.

Case	No. back-sub calls	No. decomp. calls	No. time steps
1. No reordering	55,012	11,471	33,315
2. Reordering by sunrise and sunset only	48,097	11,641	30,783
3. Full reordering	26,983	6,045	17,103

Note: In Case 1 grid cells were not reordered. In Case 2, only sunrise and sunset cells were sequestered and reordered. Finally, in Case 3, all cells were reordered and sunrise and sunset cells were both sequestered and reordered.

drawn from Atkinson *et al.* (1992), Gery *et al.* (1989), DeMore *et al.* (1990), Paulson and Seinfeld (1992), and references therein. The reaction list is available, along with SMVGEAR II, via the internet, as described on the first page of this article.

SMVGEAR II solves any number of chemical mechanisms during the same model simulation; however, it requires only one input reaction data set. Reactions for a specific region or for several regions of the atmosphere are denoted, in the reaction table, by a given symbol that is read by the computer. In addition, SMVGEAR II allows different atmospheric regions to be chosen arbitrarily and grid cells to be reordered in each region automatically. For the simulations discussed here, regions of the atmosphere below 900 mb were considered urban regions, regions between 900 and 225 mb were considered free tropospheric regions, and regions between 225 and 1 mb were considered stratospheric regions. However, these assignments are easily changed.

While different reactions are solved in different regions of the atmosphere, all species are permitted to be transported throughout all regions of the atmosphere. In other words, when chemistry and radiation are coupled to horizontal and vertical transport (e.g. advection and convection), all species in the master list are permitted to travel to and from each region of the atmosphere. However, different sets of chemical reactions affect the species in each region.

At least two reasons exist for using different reaction sets for different atmospheric regions. First, many reactions are unimportant in some regions of the atmosphere. For example, oxygen, nitrous oxide, water, and chlorofluorocarbon photolysis occur in the stratosphere but not in the troposphere, and aromatic hydrocarbons play a relatively minor role in stratospheric photochemistry. With one reaction set, numerous excess computations are required if all reactions are included in all regions of the atmosphere. Thus, dividing the atmosphere into regions where photochemical mechanisms differ reduces computer time substantially.

Similarly, dividing up the atmosphere allows intense treatment of chemistry in one or more region of the atmosphere while allowing other regions of less concern to be treated less rigorously. Thus, a modeler interested primarily in the troposphere can solve tropospheric chemistry in detail but simplify stratospheric chemistry to obtain reasonable boundary condition concentrations. Similarly, a modeler interested primarily in the stratosphere can solve stratospheric chemistry in detail but simplify tropospheric chemistry.

3. TIMINGS OF SMVGEAR II OVER A GLOBAL DOMAIN

3.1. *Setup of simulations*

To test the speed of SMVGEAR II, simulations of chemistry coupled to radiative transfer over two global grids were performed on a Cray 90 supercomputer. Both grids had

horizontal resolution 3.91 × 5° (46 latitudinal and 72 longitudinal grid cells) and used spherical coordinates. However, one grid used 15 vertical layers and the other used 29 vertical layers (sigma coordinates). Thus, the first grid required 49,680 grid cells and the second required 96,048 grid cells. Both grids were similar to those used in the UCLA Atmospheric General Circulation Model.

For the 15-layer model, nine layers were defined above 225 mb, five layers were defined between 225 and 900 mb, and one layer was defined below 900 mb. For the 29-layer model, 18 layers were defined above 225 mb, 10 layers were defined between 225 and 900 mb, and one layer was defined below 900 mb. Urban chemistry was solved for in grid cells below 900 mb, free tropospheric chemistry was solved for in cells between 225 and 900 mb, and stratospheric chemistry was solved for in cells above 225 mb.

The radiation fields in the model were determined in the following manner. First, zenith angles, time of sunrise, and time of sunset for each grid cell were determined using formulas from the Astronomical Almanac (Nautical Almanac Office, 1993). Second, absorption cross section and quantum yield data for all radiative species were compiled. Third, a wavelength grid was set up that consisted of 87 intervals between 175 and 800 nm. Fourth, ultraviolet and visible optical depths for each wavelength were determined for each grid cell by accounting for Rayleigh scattering and gas absorption. Aerosol scattering and absorption were ignored for these simulations.

Optical depths for each grid cell were determined by multiplying extinction coefficients by the thickness of the cell. Spectral extinction by gas absorption was calculated by summing, over all photodissociating gases, the product of the gas' absorption cross section at each wavelength and its number concentration. Since number concentrations varied in time due to changing chemistry, optical depths also varied in time due to chemistry. Consequently, a feedback was created between chemistry and radiation. In this feedback, chemistry affected concentrations, which affected optical depths, which affected radiation fields, which affected chemistry.

Next, optical depth, single-scattering albedo, and zenith angle information was used to calculate mean intensities. To solve for mean intensities, the tridiagonal, radiative transfer solution technique of Toon *et al.* (1989) was used. Mean intensities, absorption cross sections, and quantum yield data were then used to calculate photolysis rates for the beginning and end of each chemistry time interval. During each interval, photolysis rates at the beginning and end of the interval were interpolated to find an approximate rates during each integration time step. Thus, the model determined global radiation fields that varied in time and space.

Finally, initial meteorological conditions and gas mixing ratios were needed. Standard vertical temperature and pressure profiles (NOAA, 1976) were set uniformly over the globe to simplify the simulations. Similarly, vertical gas mixing ratio profiles were initially uniform, but varied significantly during the model simulations due to time- and space-varying radiation fields. Initial vertical profiles of NO, NO_2, N_2O, HNO_3, H_2O, O_3, OH, HO_2, H_2O_2, HO_2NO_2, CO, CH_4, HCl, $ClONO_2$, CH_3Cl, CCl_4, $CFCl_3$, CF_2Cl_2, ClO, and HOCl were interpolated from Brasseur and Solomon (1986). Also, stratospheric bromine was taken as 17 pptv (Garcia and Solomon, 1994). In addition, surface mixing ratios of organic species and bond groups (including formaldehyde, higher aldehydes, acetone, ketones, paraffins, ethene, olefins, toluene, xylene, and isoprene) were obtained from San Nicolas Island measurements on the morning of 29 August 1987 (Lurmann *et al.*, 1992). Such values were scaled with altitude. Also, mixing ratios of O_2, N_2, H_2, CO_2, and SO_2 were initialized at 20.95%, 78.08%, 0.53 ppmv, 350 ppmv, and 50 pptv, respectively.

3.2 *Computer timings*

A 30 day global simulation was run for each of the two grid sizes described in Section 3.1. Simulation A was run over the 15-layer grid (49,680 grid cells) and Simulation B was run over the 29-layer grid (96,048 grid cells). The chemistry time interval for the simulations was 30 min, and the integration time steps during each interval varied. All simulations were carried out with a relative error tolerance of 10^{-3}, which was shown in Jacobson and Turco (1994) to give a normalized gross error of 0.25% for stratospheric chemistry after 9 days. Table 2 shows timings and speeds of different SMVGEAR II processes during the two simulations. Finally, Table 3 shows the reduction in the number of operations during matrix decomposition and back substitution for each of the urban, free tropospheric, and stratospheric chemical reaction sets.

Table 2 shows that SMVGEAR II required 6.2 h on a single processor of a C-90 to solve the photochemistry for Simulation A and 11.62 h to solve the photochemistry for Simulation B. The table also shows that grid-cell reordering and photolysis interpolation required very little time in comparison to other SMVGEAR II processes. The driver routine required the most time; however, no single subroutine dominated computer time. Note that the average megaflop speed

Table 2. Statistics from two global chemistry simulations of SMVGEAR II on a Cray 90 supercomputer

	Simulation A			Simulation B		
Process	Time (h)	% of total time	Speed (mflops)	Time (h)	% of total time	Speed (mflops)
Driver routine	1.62	26.2	408.8	3.03	26.1	403.3
First derivative evaluation	1.38	22.2	324.2	2.54	21.9	321.6
Matrix back substitution	1.09	17.6	426.3	2.01	17.3	420.5
Matrix decomposition	0.71	11.5	401.1	1.35	11.6	395.8
Partial derivative evaluation	0.63	10.1	328.0	1.21	10.4	324.2
Kinetic rate constant calculation	0.53	8.5	311.9	0.98	8.4	312.0
Grid cell reordering	0.16	2.6	68.9	0.34	2.9	68.7
Photolysis interpolation	0.08	1.3	352.7	0.16	1.4	351.2
Total time/average speed	6.20	100%	366.2	11.62	100%	361.2

Note: Simulations A and B were for 30 day. For Simulation A, photochemistry was integrated in 49,680 grid cells (15-layer global model) and for Simulation B, photochemistry was integrated in 96,048 grid cells (29-layer model). Radiation fields were calculated explicitly over the globe, and three chemistry reaction sets were used, as described in the text. Radiation field calculation timings were separated out; thus the timings and speeds shown here are for photochemical calculations only. *Photolysis interpolation* means the interpolation of photolysis rates between the beginning and end of each time interval.

Table 3. Reduction in array space and in the number of matrix operations before and after the use of sparse-matrix techniques.

	Urban			Free troposphere			Stratosphere		
		After sparse matrix reductions			After sparse matrix reductions			After sparse matrix reductions	
	Initial	Day	Night	Initial	Day	Night	Initial	Day	Night
Order of matrix	94	94	94	74	74	74	43	43	43
No. init. matrix positions filled	8836	735	712	5476	585	565	1849	292	267
% of initial positions filled	100	8.3	8.1	100	10.7	10.3	100	15.8	14.4
No. final matrix positions filled	8836	897	875	5476	728	710	1849	337	298
% of final positions filled	100	10.2	9.9	100	13.3	13.0	100	18.2	16.1
No. operations decomp. 1	272,459	1978	1894	132,349	1709	1627	25,585	709	581
No. operations decomp. 2	4371	458	440	2701	361	346	903	147	118
No. operations back-sub. 1	4371	458	440	2701	361	346	903	147	118
No. operations back-sub. 2	4371	345	341	2701	293	290	903	147	137

Note: Cases are shown for urban, free tropospheric, and stratospheric chemistry. The last four rows of the table indicate the number of operations in each of four loops of matrix decomposition and back substitution. *Decomp.* 1 and 2 refer to the first and second loops occurring during each decomposition call, and *back sub.* 1 and 2 refer to the first and second loops occurring during each back-substitution call. The first column in each case shows values without sparse-matrix reductions, and the second two columns in each case show values with the reductions, for each day and night chemistry.

of SMVGEAR II, as shown in Table 2, was about 11.5% faster than the speed of SMVGEAR, as shown in Table 4 of Jacobson and Turco (1994). The difference in speed resulted from line-by-line vectorization improvement in several subroutines of SMVGEAR II.

Table 3 shows the savings in the number of matrix operations that resulted from breaking the grid domain into three distinct regions. For example, suppose, the urban chemical mechanism were used for the entire grid instead of for regions below 900 mb. In such a case, the first loop of matrix decomposition would require 1200 more operations for each stratospheric grid cell and 250 more operations for each free-tropospheric cell than it currently does, increasing computer time significantly.

Thus, SMVGEAR II is faster than SMVGEAR in three respects: (1) SMVGEAR II requires fewer total operations due to reordering, (2) individual loops in SMVGEAR II are more efficient due to improved vectorization, and (3) SMVGEAR II allows different chemical mechanisms to be solved for in different regions of the atmosphere, reducing computations for unimportant reactions in some regions.

4. CONCLUSION

A solver of first-order, ordinary differential equations over large grid domains (SMVGEAR) was modified in two ways to produce SMVGEAR II. First, grid cells were reordered according to stiffness each chemistry time interval. Stiffness was estimated with a predictor equation for all grid cells, except for sunrise cells. For sunrise cells, stiffness was predicted by time of sunrise. For both sunrise and sunset cases, cells were sequestered and solved together in their own grid blocks. Reordering of grid cells improved speeds by a factor of more than two compared to not reordering. Second, SMVGEAR was modified to allow the serial solution of any number of gas-chemistry sets during the same model run. For the simulations shown here, 200 *urban* chemical reactions were solved for in regions of the atmosphere below 900 mb, 169 *free-tropospheric* reactions were solved for in regions between 900 and 225 mb, and 115 *stratospheric* reactions were solved for in regions above 225 mb.

Computer timings of two global simulations were shown. First, a 30 day simulation of chemistry over a global 15-layer grid (49,680 grid cells) required 6.2 h of computer time for chemistry on a C-90 computer. Second, a 30 d simulation over a global 29-layer grid (96,048 grid cells) required 11.6 h. The average speed of the chemistry algorithms was over 360 megaflops. For these simulations, chemistry was coupled interactively with radiative transfer. In sum, SMVGEAR II—a variable order, iterative solver—was able to compute detailed photochemistry efficiently over a global grid when radiation fields changed continuously in time and space and when the effects of chemistry and radiation fed back to each other.

Acknowledgement—Cray Research, Inc. supported the use of an EL98 and J916 computer. Also, both the San Diego Supercomputer Center and the EPA Supercomputer Center at Bay City, Michigan permitted the use of a C90 computer. Finally, this work was supported, in part, by a grant from the Environmental Protection Agency. Although the research described in this article has been funded in part by the United States Environmental Protection Agency under assistance agreement 823755-01-0, it has not been subjected to the Agency's peer and administrative review and therefore may not necessarily reflect the views of the Agency and no official endorsement should be inferred.

REFERENCES

Atkinson R., Baulch D. L., Cox R. A., Hampson Jr. R. F., Kerr J. A. and Troe J. (1992) Evaluated kinetic and photochemical data for atmospheric chemistry. Supplement IV. *J. phys. chem. Ref. Data* **21**, 1125–1571.

Austin J. (1991) On the explicit versus family solution of the fully diurnal photochemical equations of the stratosphere. *J. geophys. Res.* **96**, 12,941–12,974.

Brasseur G. and Solomon S. (1986) *Aeronomy of the Middle Atmosphere*. D. Reidel, Dordrecht.

Byrne G. D., Hindmarsh A. C., Jackson K. R. and Brown H. G. (1977) A comparison of two ODE codes: GEAR and EPISODE. *Comput. chem. Engng* **1**, 133–147.

Crutzen P. J., Isaksen I. S. A. and McAfee J. R. (1978) The impact of the chlorocarbon industry on the ozone layer. *J. geophys. Res.* **83,** 345.

DeMore W. B., Sanders S. P., Golden D. M., Molina M. J., Hampson R. F., Kurylo M. J., Howard C. J. and Ravishankara A. R. (1990) Chemical kinetics and photochemical data for use in stratospheric modeling. Evaluation number 9. Rep. 90-I. Jet Propul. Lab., Pasadena, California.

Derwent R. G. (1982) Two-dimensional model studies of the impact of aircraft exhaust emissions on tropospheric ozone. *Atmospheric Environment* **16,** 1997–2007.

Elliott S., Shen M., Dao C. Y. J., Turco R. P. and Jacobson M. Z. (1995) A streamlined family photochemistry module reproduces major nonlinearities in the global tropospheric ozone system. *Comput. Chem.* in press.

Garcia R. R. and Solomon S. (1983) A numerical model of the zonally averaged dynamical and chemical structure of the middle atmosphere. *J. geophys. Res.* **88,** 1379.

Garcia R. R. and Solomon S. (1994) A new numerical model of the middle atmosphere 2. Ozone and related species. *J. geophys. Res.* **99,** 12,937–12,951.

Gear C. W. (1971) *Numerical Initial Value Problems in Ordinary Differential Equations.* Prentice-Hall, Englewood Cliffs, New Jersey.

Gery M. W., Whitten G. Z., Killus J. P. and Dodge M. C. (1989) A photochemical kinetics mechanism for urban and regional scale computer modeling. *J. geophys. Res.* **94,** 12,925–12,956.

Hindmarsh A. C. (1983) ODEPACK, a systematized collection of ODE solvers. In *Scientific Computing* (edited by Stepleman R. S. *et al.*), pp. 55–74. North-Holland, Amsterdam.

Hough A. M. (1991) The development of a two-dimensional tropospheric model: The model chemistry. *J. geophys. Res.* **96,** 7325–7362.

Isaksen I. S. A. and Hov O. (1987) Calculations of trends in the tropospheric concentrations of O_3, OH, CO, CH_4, and NO_x. *Tellus* **39B,** 271–285.

Jacob D. J., Sillman S., Logan J. A. and Wofsy S. C. (1989) Least independent variables method for simulation of tropospheric ozone. *J. geophys. Res.* **94,** 8497–8509.

Jacobson M. Z. (1994) Developing, coupling, and applying a gas, aerosol, transport, and radiation model to study urban and regional air pollution. Ph.D. thesis, Dept of Atmospheric Sciences, University of California, Los Angeles.

Jacobson M. Z. and Turco R. P. (1994) SMVGEAR: A sparse-matrix, vectorized Gear code for atmospheric models. *Atmospheric Environment* **28A,** 273–284.

Kanakidou M., Singh H. B. and Crutzen P. J. (1991) A two-dimensional study of ethane and propane oxidation in the troposphere. *J. geophys. Res.* **96,** 15,395–15,413.

Kao C-Y. J., Glatzmaier G. A., Malone R. C. and Turco R. P. (1990) Global three-dimensional simulations of ozone depletion under post-war conditions. *J. geophys. Res.* **95,** 22,495–22,512.

Kaye J. A. and Rood R. B. (1989) Chemistry and transport in a three-dimensional stratospheric model: chlorine species during a simulated stratospheric warming. *J. geophys. Res.* **94,** 1057–1083.

Ko M. K. W., Schneider H. R., Shia R.-L., Weisenstein K. and Sze N.-D. (1993) A two-dimensional model with coupled dynamics, radiation, and photochemistry 1. Simulation of the middle atmosphere. *J. geophys. Res.* **98,** 20,429–20,440.

Lefevre F., Brasseur G. P., Folkins I., Smith A. K. and Simon P. (1994) Chemistry of the 1991–1992 stratospheric winter: Three-dimensional model simulations. *J. geophys. Res.* **99,** 8183–8195.

Logan J. A., Prather M. J., Wofsy S. C. and McElroy M. B. (1981) Tropospheric chemistry: A global perspective. *J. geophys Res.* **86,** 7210–7254.

Lurmann F. W., Main H. H., Knapp K. T., Stockburger L., Rasmussen R. A. and Fung K. (1992) "Analysis of the ambient VOC data collected in the Southern California Air Quality-Study." Final Report to the California Air Resources Board under contract No. A832–130, 1992.

Nautical Almanac Office and Her Majesty's Nautical Almanac Office (1993) Astronomical Almanac. U.S. Government Printing Office, Washington, District of Columbia.

NAS (1992) *NAS User Guide,* Vol. 2, Version 6.0, Section 4, p. 22. Moffett Field, California.

NOAA (1976) U.S. Standard Atmosphere. Washington, District of Columbia.

Paulson S. E. and Seinfeld J. H. (1992) Development and evaluation of a photooxidation mechanism for isoprene. *J. geophys. Res.* **97,** 20,703–20,715.

Press W. H., Flannery B. P., Teukolsky, S. A. and Vetterling W. T. (1992) *Numerical Recipes: The Art of Scientific Computing.* Cambridge University Press, Cambridge.

Rose K. and Brasseur G. (1989) A three-dimension model of chemically active trace species in the middle atmosphere during disturbed winter conditions. *J. geophys. Res.* **94,** 16,387–16,403.

Strand A. and Hov O. (1994) A two-dimensional global study of tropospheric ozone production. *J. geophys. Res.* **99,** 22,877–22,895.

Tie X., Lin X. and Brasseur G. (1994) Two-dimensional coupled dynamical/chemical/microphysical simulation of global distribution of El Chichon volcanic aerosols. *J. geophys. Res.* **99,** 16,779–16,792.

Toon O. B., McKay C. P. and Ackerman T. P. (1989) Rapid calculations of radiative heating rates and photodissociation rates in inhomogeneous multiple scattering atmospheres. *J. geophys. Res.* **94,** 16,287–16,301.